ISSN 1063-7834, Physics of the Solid State, 2018, Vol. 60, No. 11, pp. 2173–2177. © Pleiades Publishing, Ltd., 2018.
Original Russian Text © N.V. Kinev, K.I. Rudakov, A.M. Baryshev, V.P. Koshelets, 2018, published in Fizika Tverdogo Tela, 2018, Vol. 60, No. 11, pp. 2132–2136.

SEMICONDUCTORS

Slot Lens Antenna Based on Thin Nb Films for the Wideband Josephson Terahertz Oscillator

N. V. Kinev[a, *], K. I. Rudakov[a, b, c], A. M. Baryshev[c], and V. P. Koshelets[a]

[a] *Kotel'nikov Institute of Radio Engineering and Electronics, Russian Academy of Science, Moscow, 125009 Russia*
[b] *Moscow Institute of Physics and Technology, Dolgoprudny, 141701 Russia*
[c] *University of Groningen, 9712 CP Groningen, Netherlands*
**e-mail: nickolay@hitech.cplire.ru*

Received May 14, 2018

Abstract—An oscillator based on the distributed tunnel superconductor-insulator-superconductor junction with an ultrawide operating bandwidth of up to 100% of the central frequency seems to be a promising type of directional source of continuous electromagnetic radiation in the terahertz frequency range. In this paper, we propose a scheme of a terahertz oscillator integrated on a single microchip with a transmitting lens antenna with the slot structure in a 200-nm Nb film to radiate the signal into the open space. We also proposed and numerically simulated several designs of a planar slot antenna matched (in the input) with a Josephson oscillator and (in the output) with a silicon elliptical lens. The obtained results of the matching of the oscillator output power with the antenna of various designs operating in four frequency ranges: 250–410, 330–570, 380–520, and 420–700 GHz are presented. The antenna beam patterns and impedances are calculated as well.

DOI: 10.1134/S1063783418110112

1. INTRODUCTION

The lack of broadband sources in the terahertz (THz) frequency range is a big scientific problem at present. The THz-band oscillator based on the Nb/AlO_x/Nb or Nb/AlN/NbN distributed tunnel junction is successfully used as the reference heterodyne in the 450–650 GHz superconductor integrated receiver (SIR) [1–3]. In this case, the frequency tuning range of the oscillator is much wider while the SIR operating range is determined by both the bandwidth of the quasi-optical planar lens antenna and the matching transmission lines between the local oscillator and the superconductor-insulator-superconductor (SIS) mixer. Thus, to date, the emission range of a Nb/AlN/NbN oscillator with dimensions of 400 × 16 μm^2 is from 200 to 750 GHz (bandwidth is about 100% of the central frequency) with a spectral line width of the order of 1 MHz. In this case, the upper limit the emission range is limited to half the energy gap of the superconductor forming the transmission line and can potentially be up to 1 THz. To stabilize the radiation frequency and synchronize the power in the central peak, a phase locked loop (PLL) is used that narrows the actual line width to about 40 kHz and collects up to 97% of the radiation power in the peak. This oscillator has a relatively low output power of fractions to units of microwatts, which is nevertheless sufficient for a wide range of problems. Such problems also include the heterodyne detection in the THz range, where pumping of SIS mixers or HEB (hot electron bolometer) mixers requires power in fractions of microwatts, as well as laboratory spectroscopy of gases.

To date, the Josephson oscillator based on a single distributed SIS junction was exclusively used as part of integrated receiver circuits as a reference oscillator for pumping a sensitive element. In such circuits, the oscillator and mixer are placed on a single chip and matched by microstrip and coplanar transmission lines. This application is very convenient from a technical point of view since it does not require an external source of the heterodyne.

To our best knowledge, there are no studies with attempts to develop an oscillator to the open space based on a distributed SIS junction for practical applications yet. Such studies seem reasonable and interesting from a practical point of view, since the oscillator has an ultrawide operating band, it is easy enough to operate and relatively inexpensive in manufacturing compared to other THz sources, and has enough power to solve many problems. A transmitting antenna-lens system matched with the oscillator is used to output the oscillator emission to the open space. In this paper, we calculated antenna-lens systems that operate in the frequency range from 250 to 700 GHz.

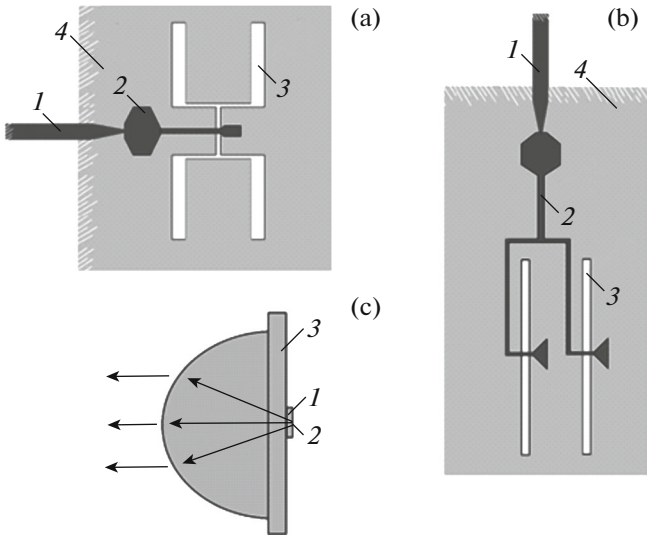

Fig. 1. (a, b) Are a schematic representation of the planar integrated structure of (*1*) the THz oscillator based on the distributed SIS transition matched by (*2*) the microstrip line to (*3*) the slot antenna. The slot structure is realized in (*4*) the metallization layer, which is also the lower electrode of the microstrip line; (c) is a schematic representation of (*1*) a microcircuit with a planar integrated structure of the oscillator and (a) or (b) antenna placed in (*2*) the far focus of (*3*) the silicon lens. (Figure (c) is not drawn to scale.)

2. THE CONCEPT OF A THz OSCILLATOR INTEGRATED WITH A LENS ANTENNA

The key idea of the oscillator design is the integration of the oscillator with the transmitting slot antenna on a single chip (Figs. 1a and 1b). The microcircuit is placed on the surface of a collecting elliptical lens made of silicon, so that the antenna is in the lens focus (Fig. 1c). The substrate material of the chip and the lens is chosen to be the same, i.e., silicon with a dielectric constant of $\varepsilon = 11.7$, in order to avoid refraction of the beams inside the system design. Thus, the main problem is both to match the power of the oscillator with a low output impedance (fractions of Ω) and a quasi-optic lens antenna with a relatively high impedance (tens of Ω), and to create the required directional diagrams.

The operational principle of the oscillator based on the distributed SIS junction is described in detail elsewhere [4–6]. A unidirectional flux of magnetic flux vortices (fluxons) is produced in this junction under the effect of an external magnetic field and a bias current. The characteristic size of the fluxon is of the order of the double Josephson penetration depth of $2\lambda_J$, which is about 8 μm at a characteristic current density of the order of 5 kA/cm^2. The condition for the junction distribution is that the junction size in the direction of fluxon propagation (a length of L) is much larger than the fluxon size, that is, $L \gg 2\lambda_J$. The characteristic length of these oscillators ranges from 300 to 700 μm at the W width from 3 to 20 μm. In this study, we use an oscillator identical to the reference oscillator in SIR with dimensions of 400 × 16 μm^2 for antennas with a operating range of above 400 GHz while a 700-μm junction is chosen for operation in a frequency range of below 400 GHz. The junction will be based on three-layer Nb/AlO_x/Nb or Nb/AlN/NbN SIS structures with a current density of ~2–5 kA/cm^2. The Josephson oscillator is a voltage-controlled oscillator, and the f oscillator frequency is determined by the fundamental Josephson relation:

$$hf = 2eV_{DC},$$

where V_{DC} is the DC voltage at the junction. A control line of a magnetic field is used to produce a magnetic field in the junction region. The control line is structurally the lower superconducting niobium electrode, through which a direct current passes.

The design of the two types of the developed slot antenna is shown schematically in Figs. 1a and 1b (element *3*). A slot antenna of the first type (Fig. 1a) was used earlier [7] as a receiving lens antenna of an SIS receiver at central frequencies of 100, 246, and 500 GHz while the microcircuit with the antenna was also mounted on the silicon lens. This geometry of the planar antenna was chosen in this study as the first attempt to match the oscillator based on a flux of Josephson vortices with an open space. An antenna of this type has a narrower band than the oscillator used, so the necessary operating range of 250–700 GHz is realized by three geometric antenna designs with a central frequency of 350, 450, and 600 GHz. The antenna designs differ in geometric dimensions of the elements (length and width of the four "cut-outs" and the connection between them, the distance between the "cut-outs"), as well as the topology of the microstrip transmission line (Fig. 1a, element *2*), including the impedance transformer. A second type of the proposed slot antenna is operating at a central frequency of 450 GHz coinciding with the central frequency of one of the three previously designated structures. An antenna of the second type (Fig. 1b) was also used earlier [8] as a receiving lens antenna in the 500-GHz SIS receiver while an SIS mixer with an impedance of ~4 Ω was included in a microstrip line. All slot antenna designs are realized in thin Nb films with a thickness of ~ 200 nm. An elliptical silicon lens with an ellipse width of 10 mm was chosen as a collecting lens for all antenna designs. Precisely this lens was used in the SIP as a part of the TELIS instrument for studying the spectra of atmospheric gases in the 450–650 GHz range in the scanning mode at an altitude of 20–35 km [2]. The value of the thickening over the semi-ellipse of the lens with allowance for the silicon substrate thickness of 0.535 mm is chosen such that the far focus of the ellipse falls exactly on the antenna plane. It was shown that this lens with allowance for the arrangement of a matched antenna in its focus can

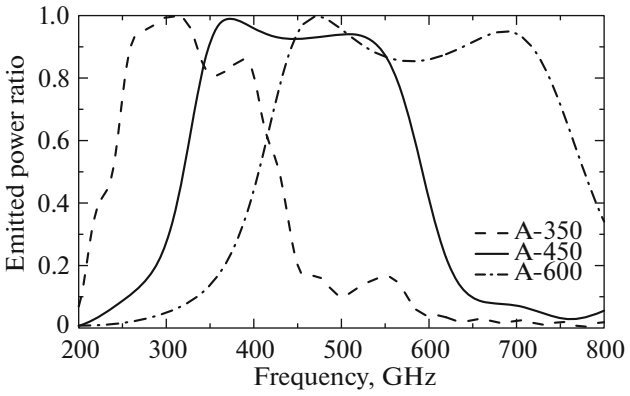

Fig. 2. Percentage of the power emitted by the antenna of the first type of three different designs to the full solid angle of 4π.

be effectively used in a wide frequency range of 0.1–1 THz without the need to change the lens geometry [7]. Since cooling is necessary for the operation of a $Nb/AlO_x/Nb$ or Nb/AlN/NbN superconductor oscillator, the entire design of the oscillator with an antenna-lens system is placed in a cryogenic setup at a liquid helium temperature of 4.2 K In this case, the antenna and microstrip transmission Nb lines with a critical temperature T_c of about 9 K are also in the superconducting state.

3. NUMERICAL SIMULATIONS: POWER, IMPEDANCE, AND BEAM PATTERNS

Three-dimensional numerical simulations of the radiating antenna design were carried out by using CST Studio. The London penetration depth of the magnetic field for thin Nb films was $\lambda_L = 85$ nm. The value was used to take into account the superconducting state of the antennas and microstrip transmission lines. Figure 2 shows the calculation results of the power matching for the three antenna designs of the first type shown in Fig. 1a operated at central frequencies of 350, 450, and 600 GHz (hereinafter, the antenna designs correspond to the A-350, A-450, and A-600 curve labels). The figure also shows the frequency dependence of the radiation power percentage in the open space of the oscillator's total output power. More than 70% of the power is uniformly emitted by antennas near the central frequency in the ranges of 250–410, 330–570, and 420–700 GHz. The microstrip transmission line was designed to match the low output impedance of the oscillator, which was set to be equal to 0.5 Ω and to be frequency independent in the calculations, and the high input impedance of the quasi-optical slot antenna. Shown in Figs. 3a and 3b are the antenna impedances the first type, which were calculated for central frequencies of 450 and 600 GHz, at the point of connection to the transmission line coming from the oscillator. In both cases, the frequency dependence of the impedance within the operating range is sufficiently flat and, without jumps while the total impedance varies within 14 Ω: from 30 to 40 Ω for the 450-GHz antenna and from 26 to 40 Ω for the 600-GHz antenna. Figure 4a shows beam patterns for three antenna designs at a selected frequency near the central frequency. Most of the power is concentrated in the central lobe. Figure 4b shows a set of beam patterns for the 450-GHz antenna at frequencies of 350 to 650 GHz in 50 GHz increments. The set of diagrams at various frequencies of the operating range shows a weak frequency dependence of the radiation. It also shows the narrowest central lobe at frequencies near the central one and the diagram widening at a distance from the central frequency while the widest diagram in the considered set is at 350 and 650 GHz for the 450-GHz antenna. All the calculations were performed without taking into account the lens, adding of which to the antenna

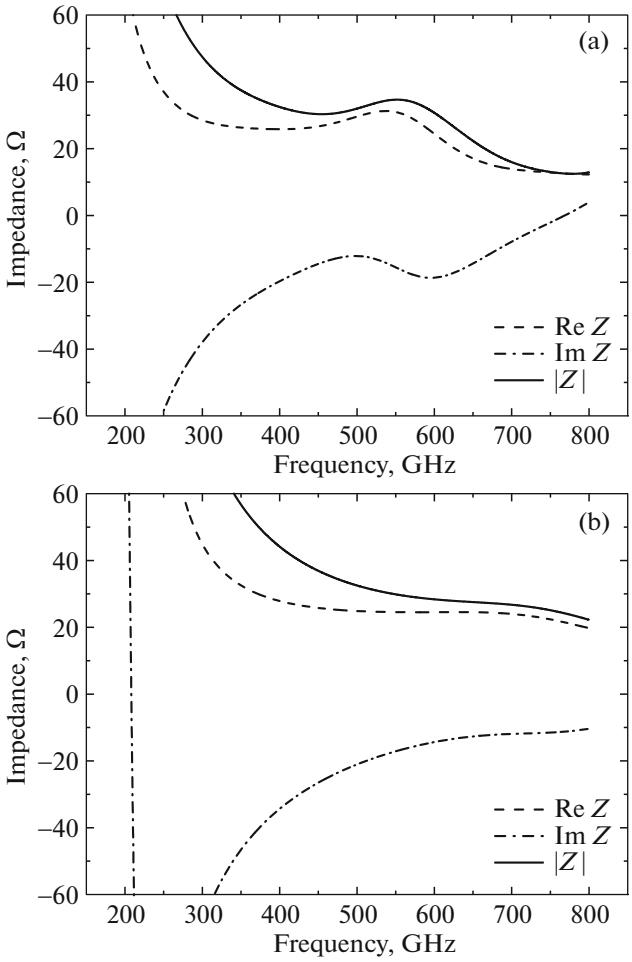

Fig. 3. (a) Impedance of the antenna for a central frequency of 450 GHz (the range of 330–570 GHz) and (b) antenna impedance for the central frequency of 600 GHz (range 420–700 GHz).

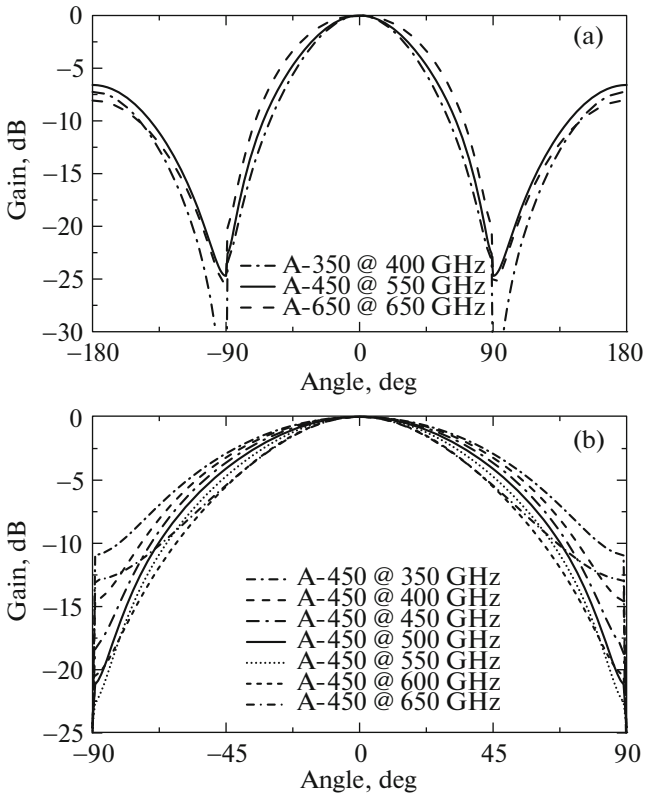

Fig. 4. (a) Beam patterns of 350-, 450-, and 600-GHz antennas at the selected frequency close to the central frequency and (b) a set of beam patterns for the 450-GHz antenna in the frequency range from 350 to 650 GHz with 50 GHz increment.

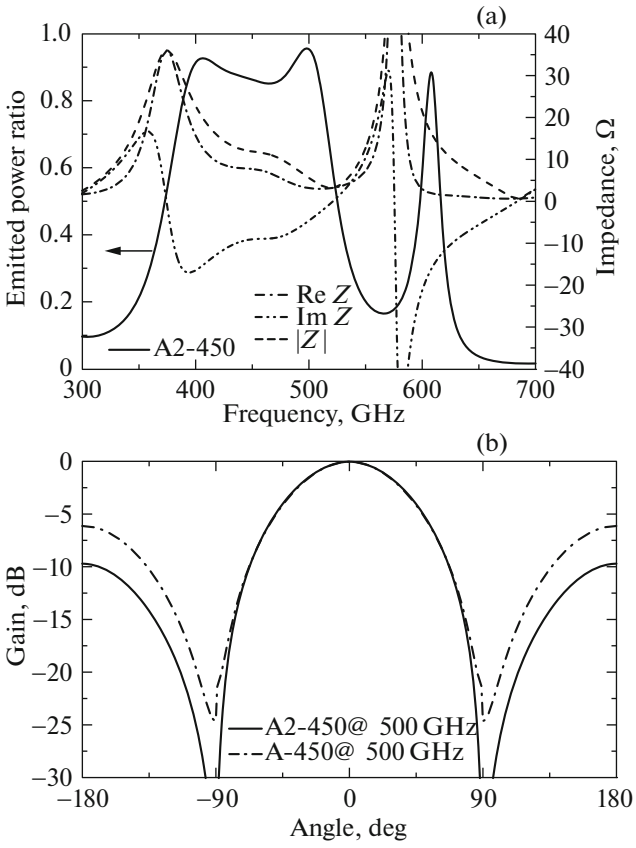

Fig. 5. (a) Frequency dependence of the percentage of emitted power (solid curve), real part of impedance (dot-and-dash line), imaginary part of impedance (dot-dash-dotted line), and module of the impedance for the antenna of the second type at a central frequency of 450 GHz (dashed line); (b) beam pattern of the antenna of the second type at a frequency of 500 GHz (solid line) in comparison with the beam pattern of the antenna of the first type at the same frequency.

reduces significantly the width and increases the power of the central lobe without affecting the power matching of the oscillator with the antenna. The total operating range of the three antenna designs of the first type ranges from 250 to 700 GHz.

The numerical calculation results for the antenna of the second type having a design shown in Fig. 1b (the antenna design is labeled on the curve as A2-450) similar to the results of the antenna of the first type at the central frequency of 450 GHz are shown in Fig. 5. The power and impedance are shown in Fig. 5a and beam pattern are show in Fig. 5b. The operating range of the antenna of the second type at the emitted power level of 0.7 was 380–520 GHz, which is by 100 GHz narrower than that for the antenna of the first type at the same central frequency of 450 GHz. The shape of the central lobe of the antenna directional diagrams is practically the same for the antennas of the both types (see Fig. 5b). However, the lobe power in the opposite direction towards the vacuum relative to the operating direction towards the substrate is by 6.5 dB lower for the antenna of the second type. Thus, the antenna of the second type is more narrow-band one and should be expected to have a larger output power in comparison with antenna of the first type.

4. CONCLUSIONS

The superconductor THz oscillator based on the unidirectional flux of Josephson vortices (fluxons) is an interesting solution of the THz source for tasks that require a wide operating frequency range and do not require high power, for example, in heterodyne detection and gas spectroscopy. The scope of applications of these tasks is extremely wide: radio astronomy and astrophysics, the Earth's atmosphere monitoring, medical diagnostic devices and security systems, technological process monitoring in manufacture, and information and telecommunication systems. In this study, we proposed the idea and practical implementation of the THz radiation output to the open space from the plane of the oscillator structure based on the

tunnel SIS junction using a slot THz antenna matched with an elliptical lens. The results of the initial stage of the study are presented: numerical simulations of the antenna and feeder structures based on microstrip transmission lines designed for frequencies of 250–410, 330–570, and 420–700 GHz; three antenna designs overlap the range of 250–700 GHz. We also presented results of the power matching of the antenna input line with an open space and calculated the beam patterns and the antenna impedances. We carried out numerical simulations of the alternative antenna design with the narrower operating range of 380–520 GHz. This antenna can be effectively implemented in practice due to its higher output power. The further work should include the fabrication of the calculated superconducting structures by magnetron sputtering and electron beam lithography and an experimental study of the developed oscillator samples. Another important area of work is to study the possibility of stabilizing the frequency and synchronization of the radiation power in the central peak by the PLL system. For this purpose, an antenna design will be developed with the branching of a fraction of the oscillator power to the harmonic mixer included in the feedback loop with the oscillator.

ACKNOWLEDGMENTS

This work was supported by the Russian Science Foundation, project no. 17-79-20343.

REFERENCES

1. V. P. Koshelets and S. V. Shitov, Supercond. Sci. Technol. **13**, R53 (2000).
2. G. de Lange, D. Boersma, J. Dercksen, P. Dmitriev, A. B. Ermakov, L. V. Filippenko, H. Golstein, R. W. M. Hoogeveen, L. de Jong, A. V. Khudchenko, N. V. Kinev, O. S. Kiselev, B. van Kuik, A. de Lange, J. van Rantwijk, et al., Supercond. Sci. Technol. **23**, 045016 (2010).
3. V. P. Koshelets, P. N. Dmitriev, M. I. Faley, L. V. Filippenko, K. V. Kalashnikov, N. V. Kinev, O. S. Kiselev, A. A. Artanov, K. I. Rudakov, Arno de Lange, G. de Lange, V. L. Vaks, M. Y. Li, and H. Wang, IEEE Trans. Terahertz Sci. Technol. **5**, 687 (2015).
4. T. Nagatsuma, K. Enpuku, F. Iri, and K. Yoshida, J. Appl. Phys. **54**, 3302 (1983).
5. Y. Zhang, Thesis (Chalmers Univ. Technol., Gothenburg, Sweden, 1991).
6. T. van Duzer and C. W. Turner, *Principles of Superconductive Devices and Circuits*, 2nd ed. (Prentice Hall, Englewood Cliffs, NJ, 1998).
7. D. F. Filipovic, S. S. Gearhart, and G. M. Rebeiz, IEEE Trans. Microwave Theory Technol. **41**, 1738 (1993).
8. J. Zmuidzinas, IEEE Trans. Microwave Theory Technol. **40**, 1797 (1992).

Translated by A. Ivanov